PCCP

Accepted Manuscript

This is an *Accepted Manuscript*, which has been through the Royal Society of Chemistry peer review process and has been accepted for publication.

Accepted Manuscripts are published online shortly after acceptance, before technical editing, formatting and proof reading. Using this free service, authors can make their results available to the community, in citable form, before we publish the edited article. We will replace this *Accepted Manuscript* with the edited and formatted *Advance Article* as soon as it is available.

You can find more information about *Accepted Manuscripts* in the **Information for Authors**.

Please note that technical editing may introduce minor changes to the text and/or graphics, which may alter content. The journal's standard **Terms & Conditions** and the **Ethical guidelines** still apply. In no event shall the Royal Society of Chemistry be held responsible for any errors or omissions in this *Accepted Manuscript* or any consequences arising from the use of any information it contains.

PhysChemChemPhys Physical Chemistry Chemical Physics

COMMUNICATION

Heat storage properties of organic phase-change materials confined in nanospace of mesoporous SBA-15 and CMK-3

Tomosuke Kadoono[a] and Masaru Ogura*[a]

A novel-type mesoporous material encapsulating phase-change materials (PCMs) is reported concerning their implication for use of thermal energy storage devices. The composites of siliceous SBA-15 or carbonaceous CMK-3
10 mesoporous assemblies and organic PCMs could be used to make leak-free devices that retain their capabilities over many thermal cycles for heat storage/release. A confinement effect was observed that alters the thermal properties of the encapsulated PCM, especially into CMK-3 without any
15 similar effects in other carbon materials.

Mesoporous silica materials, first reported almost two decades ago, have become the focus of a great deal of recent research in the field of nanostructured materials because of their periodic structure, uniform pores, and extremely high surface areas.
20 Applications for mesoporous silica include catalysts, adsorbents, and hosts for other materials.[1,2,3] The active site sizes required for these applications are generally at the nanometer scale such as metals, metal ions, and metal clusters; therefore, the unique properties of mesoporous silica have not been fully realized
25 **(Figure 1)**.

Thermal energy storage is one of the most effective approaches to energy conservation and has been utilized in areas such as a heat control systems for power generation and industrial facilities, climate control systems for buildings, and solar energy
30 harvesting.[4] Thermal storage systems can be classified by the thermodynamic nature of the heat stored: sensible heat,[5] latent heat,[6] or the heat of a chemical reaction.[7] Sensible heat storage is the most straightforward method, so complicated equipment is seldom necessary. Liquids such as water and oil and solids such
35 as rocks are typical materials used in sensible heat storage. The storage of heat derived from chemical reactions is a more difficult model to implement in practical applications, but the thermal energy stored can be recovered easily whenever desired by simply instigating a chemical reaction.

40 The storage of thermal energy in the form of the latent heat of a phase change has the useful feature of high energy storage density within a small temperature range, i.e. the temperature difference between storing and releasing heat,[8] where the liquid-solid phase transformation takes place. This latent heat storage
45 technique is usually implemented using a suitable phase-change material (PCM). Well-known PCMs include linear chain hydrocarbons (paraffins), hydrated salts, polyethylene glycols, fatty acids, and eutectic mixtures of organic and non-organic compounds. However, there are problems associated with (i)
50 leakage of the PCMs from the thermal storage system when the PCM transforms to the liquid phase and (ii) volume changes in the PCM during and after phase changes. Some researchers have demonstrated how to overcome these problems by using a capsule[9] and porous materials[10] as containers for the PCM.
55 Encapsulation of the PCM in a confined nanospace overcomes the leakage problem, but heat transfer through the wall of the capsule is slow because typical organic encapsulating materials, and the PCMs themselves, exhibit low thermal conductivity. Some researchers have tried to modify the sizes of the capsules
60 and thicknesses of the walls to improve the thermal conductivity. For instance, microcapsules with wall thicknesses less than 1 μm and the size of which is 20−40 μm in diameter have been developed.[11, 12]

In this study, mesoporous materials comprised of a uniform
65 mesopore with a thinner wall approximately 6 nm in thickness, specifically, siliceous SBA-15 and carbonaceous CMK-3, are used as containers for organic PCMs. The mesopores in SBA-15 and CMK-3 are interconnected via micropores, an arrangement that provides better heat conduction. The high specific surface
70 areas of these mesoporous materials ($\approx$ 900 m^2/g for silica and $\approx$ 1200 m^2/g for carbon) produce better overall contact with the encapsulated PCM and improve heat recovery during the phase change. Moreover, the liquid-phase PCM is not expected to leak out because of the surface tension of the PCM in the confined
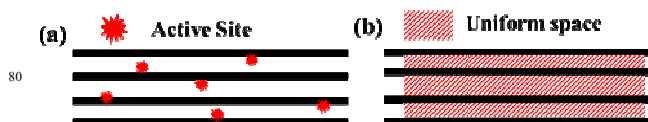75 nanospace.

85 Figure 1. Schematic images of mesoporous materials for (a) a catalyst (catalyst support) or an adsorbent, and (b) a molecular mold.

90

SBA-15 was synthesized using $EO_{20}PO_{70}EO_{20}$ (P123), a triblock copolymer, as the surfactant for producing the macromolecular micelle mesostructure and tetraethyl orthosilicate as the silica source, following the literature.[13] CMK-3 was prepared using the SBA-15 material as the hard template and sucrose as the carbon source. A 1 M NaOH solution (50 vol % ethanol + 50 vol % H_2O) was used to dissolve the silica from this C/SBA-15 composite, generating CMK-3.[14] The PCM/porous composite was fabricated using the impregnation method. The SBA-15 or CMK-3 and the selected PCM – $C_{17}H_{35}COOH$ (stearic acid (SA)) or $C_{11}H_{23}COOH$ (lauric acid (LA)) – were mixed and suspended in ethanol, after which the mixture was held at 100 °C until the ethanol evaporated.

A "German sausage" structure typical for SBA-15 was observed in SEM micrographs taken at high magnification (**Figure 2**). This tube structure remained after impregnation with the PCM/ethanol solution because SBA-15 and CMK-3 possess good thermal and chemical stability. No weight loss in any of the composites was observed during heating/cooling cycles in the temperature range tested in this study. XRD measurements also revealed that mesostructures of the hosts (SBA-15 and CMK-3) for PCM were retained after the impregnation.

Results of DSC measurements performed on SA, SA/SBA-15 (1:1), and SA/CMK-3 (1:1) are shown in **Figure 3**. All composites successfully stored and released thermal energy during melting and solidification of SA, respectively. Repetition of the temperature increase and decrease cycle (10 times) did not result in any peak position changes, indicating that the PCMs remained intact without any leakage from the mesopores or without deterioration. However, the areas (ΔH) of the endothermic and exothermic peaks decreased significantly when the PCM was incorporated into the mesoporous materials (**Table 1**). This is because the outer layer of PCM molecules adheres to the mesopore walls, which reduces the mobility of the molecule and inhibits phase changes. Even though the mobility of the adhered portion of the PCM molecule is limited, the residual space of SBA-15 is large enough for the molecule to rotate freely, since the molecular length of SA is approximately 2.0 nm and the pore size of SBA-15 is 7.6 nm. Conversely, the free space available for SA reorientation seems limited in CMK-3.
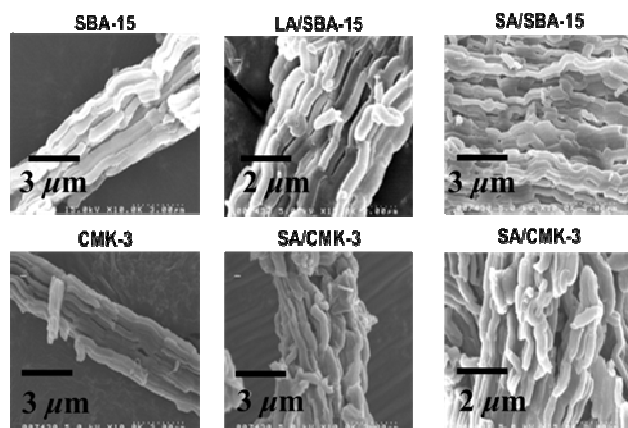

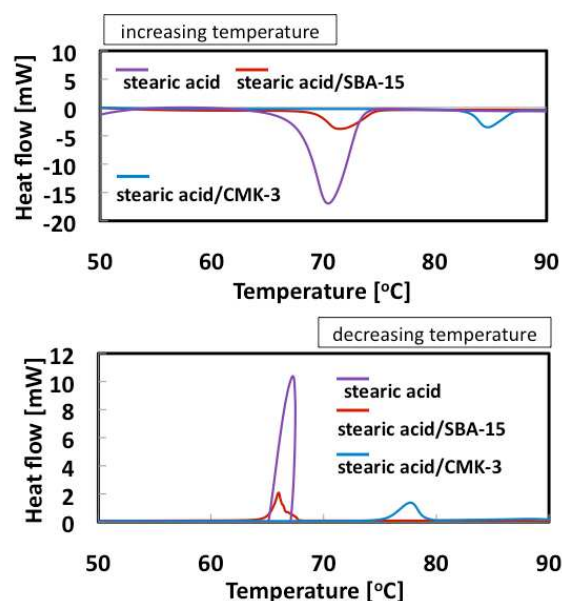Figure 2. SEM images for SBA-15 and CMK-3 materials and composites.

Figure 3. DSC curves of pure SA and the composites with SBA-15 and CMK-3.

Table 1. Thermal properties of SA and SA composites with SBA-15 and CMK-3.

Entry	M [%]	T_m [°C]	ΔH_m [J/g]	ΔH_m [J/g-SA]	$\Delta\Delta H_m$ [J/g-SA]	T_f [°C]	ΔH_f [J/g]	ΔH_f [J/g-SA]	$\Delta\Delta H_f$ [J/g-SA]
SA	100	68.8	-204	-204	-	66.5	-	211	-
SA/SBA-15 (5:5)	52.0	69.1	-36.3	-69.8	134	66.7	35.4	68.1	-143
SA/CMK-3 (5:5)	46.0	82.9	-31.5	-68.5	136	78.9	26.5	57.6	-153

It is worth noting that, as indicated by the DSC curves, the melting point of SA in CMK-3 was significantly higher than that of bulk SA and SA loaded in SBA-15. This phenomenon persisted after several heating/cooling cycles without any change in the peak area, nor any temperature shift.

The x-ray diffraction patterns (**Figure 4**) give us insight into the orientation of the PCM molecules and the assembled molecule structure. Figure 4 suggests that the crystallinity and relative diffracted intensity of the confined phase of SA were totally different than those of the bulk crystal. This indicates that crystalline structure is influenced by the limited space inside the SBA-15 and CMK-3 pores.

DSC measurements on the much shorter molecule LA, LA/SBA-15 (1:1), and LA/CMK-3 (1:1) are in **Figure 5**. Similarly to the composites incorporating SA, the LA composites could store and release thermal energy. The melting point of LA
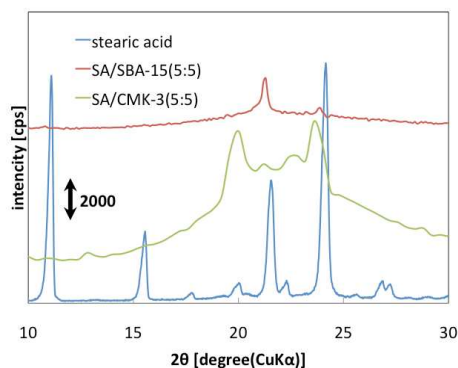
Figure 4. XRD patterns of pure SA and the composites with SBA-15 and CMK-3.

Figure 6. DSC curves of SA composites with different SA:mesoporous material ratios.

are similar to that of the bulk of PCM. Because of the pore wall
30 interaction effects, not all of the PCM incorporated into the composite underwent a phase change, thus decreasing the enthalpy of the composite overall.

It should be noted that physical mixture of the fatty acid and porous material had no effect on the temperature shift for melting
35 and solidification. These results indicate the thermal properties of PCM inside a confined space are altered. The composites possess different melting points from that of the bulk fatty acid because of the confinement effect [15, 16], and the interaction between the PCM and pore wall. An interaction between the PCM and silanol
40 on silica might play an important role in stabilizing PCM in the mesopore. Furthermore, the porous structure was a dominant factor in determining the melting point of fatty acid because the conditions around the fatty acid were non-uniform. Such a large temperature shift was not observed on the composites with SA
45 using different types of carbonaceous compound such as carbon tube, graphitic carbon, amorphous carbon, and so on.

In summary, a solid composite consisting of a PCM confined in a mesoporous material with uniform nanospaces was prepared. Storage and release of latent heat by solid/liquid phase
50 transformations of the PCM was observed when the composition ratio of PCM/mesoporous material was greater than 5:5. No leakage of liquid PCM from the mesopores was observed. Unfortunately, the heat stored in the confined PCM was lower than that of the bulk PCM because of the strong interactions
55 between the PCM molecules and the pore wall, which severely restrict their freedom of motion. An interesting effect was found whereby confinement of fatty acids in carbonaceous CMK-3 structures increases the melting point of the acid. This composite can be used in applications where the PCM should remain solid at
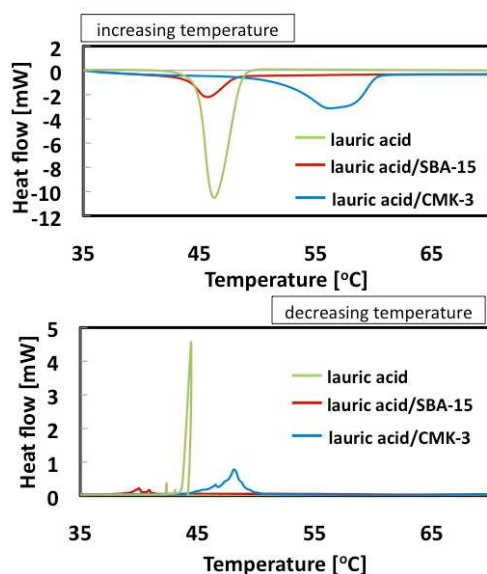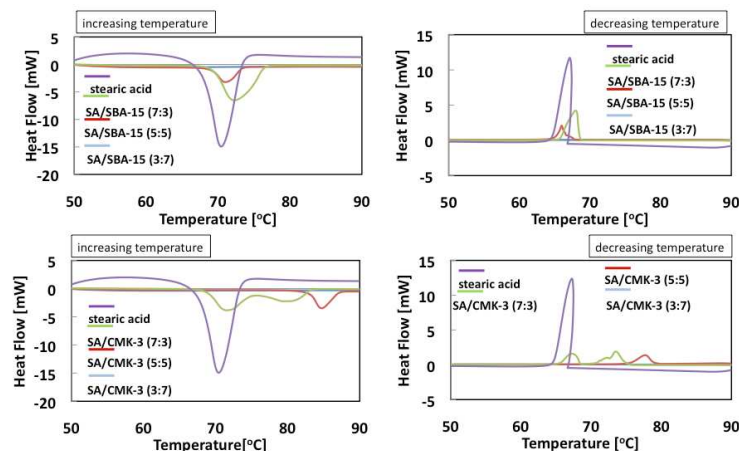60 higher temperatures.

5 Figure 5. DSC curves of pure LA and the composites with SBA-15 and CMK-3.

in CMK-3 was elevated compared to bulk LA and LA/SBA-15. Interestingly, this temperature shift was less than was the case for
10 SA/CMK-3, and a broadened peak was clearly present in both the exothermic and endothermic spectra. These results suggest that the interaction between the carbonaceous pore walls of CMK-3 and the fatty acid is different from that between the siliceous pore walls of SBA-15.

15 The latent heat produced during phase change increased with increasing PCM content in the composites with 30 to 70 wt% PCM (**Figure 6**). Similar results were obtained with LA as the PCM. For the PCMs composited with both SBA-15 and CMK-3, the exothermic and endothermic peaks disappeared at the 3:7
20 composition ratio. This phenomenon can also be explained by the interaction between PCM and mesopore wall; the minority component PCM is mostly spread onto the surface of mesopore wall, and the freedom of motion required for phase changes is severely restricted. In the case of the composites with more PCM
25 than mesoporous material, the composite transition temperatures

Experimental Section

SBA-15 material was prepared using triblock copolymer, EO$_{20}$PO$_{70}$EO$_{20}$ (Pluronic P123, BASF) as the surfactant for
65 cylindrical micelle mesostructure and tetraethyl orthosilicate (TEOS, WAKO) as the silica source. The starting composition was 1.09 g of P123, 59.9 g of HCl solution (2 mol/L, WAKO),

and 14.9 g of H_2O; this mixture was stirred at 35 °C with a magnetic stirrer until the P123 was completely dissolved. Next, 4.28 g of TEOS was added to the homogeneous solution, and this slurry was stirred for 20 h at 35 °C. The resultant mixture was placed in an air oven for 24 h at 100 °C. Then the product was filtered, washed with water, dried at 100 °C overnight, and calcined at 550 °C in flowing air. Surface area, mesopore volumes, and the mesopore diameter of the obtained SBA-15 were 931 m^2/g, 1.04 cm^3/g, and 7.6 nm, respectively.

CMK-3 material was prepared using SBA-15 as the hard template, sucrose as the carbon source, and sulfuric acid as the acid catalyst. 1.09 g of calcined SBA-15 was added to a solution composed of 1.25 g of sucrose (WAKO) and 0.15 g of H_2SO_4 (WAKO) in 5.01 g of H_2O. The mixture was kept within a tightly sealed vessel in an air oven for 6 h at 100 °C, then the temperature was increased to 160 °C for 6 h. The sample was treated at these conditions again after adding 0.81 g of sucrose, 0.09 g of H_2SO_4, and 4.98 g of H_2O. Carbonization was carried out by pyrolyzing sucrose at 800 °C in flowing N_2. The resultant carbon-silica composite was washed with 1 M NaOH solution (50 vol % ethanol-50 vol % H_2O) twice at 100 °C. The template-free carbon was filtered, washed with ethanol, and dried at 100 °C. Surface area, mesopore volumes, and the mesopore diameter of the obtained CMK-3 were 1210 m^2/g, 0.76 cm^3/g, and 3.5 nm, respectively.

The PCM/porous material composite was fabricated using an impregnation method. 30, 50, and 70 mg of porous material (SBA-15 or CMK-3), and the same weight of PCM (stearic acid or lauric acid) were mixed, along with an aliquot of ethanol. The mixture was held for 24 h at 100 °C to remove the ethanol.

The field emission scanning electron microscopic study was performed with a Hitachi High-Technologies S-4500. This instrument was operated at an electron acceleration voltage of 10 kV when observing the composite structures. TG-DTA was performed with Rigaku Thermoplus TG8120. These composites were heated under air flow at a rate of 10 K/min to 1000 °C. DSC was performed with Rigaku Thermoplus EVO II DSC8230 instrument. These composites were heated and cooled (35°C-70°C-35°C, 50°C-90°C-50°C) at a rate of 5 K/min.

Acknowledgements

Notes and references

^{a} Institute of Industrial Science, The University of Tokyo, Komaba 4-6-1, Meguro, Tokyo, Japan. Fax: 81 3 5452 6322; Tel: 81 3 5452 6321; E-mail: oguram@iis.u-tokyo.ac.jp

† Electronic Supplementary Information (ESI) available: [details of any supplementary information available should be included here]. See DOI: 10.1039/b000000x/

1 H.H.P. Yiu, C.H. Botting, N.P. Botting and P.A. Wright, *Phys. Chem. Chem. Phys.*, 2001, **3**, 2983.

2 K. Sugino, N. Oya, N. Yoshie and M. Ogura, *J. Am. Chem. Soc.*, 2011, **133**, 20030.

3 K. Ariga, A. Vinu, Y. Yamauchi, Q. Li and J.P. Hill, *Bull. Chem. Soc. Jpn.*, 2012, **85**, 1.

4 B. Zalba, J.M. Marin, L.F. Cabeza and H. Mehling, *Appl. Thermal Eng.*, 2003, **23**, 251.

5 I. Dincer, S. Dost and X. Li, *Int. J. Energy Res.*, 1997, **21**, 1157.

6 H. Ettouney, H. El-Dessouky and E. Al-Kandari, *Ind. Eng. Chem. Res.*, 2004, **43**, 5350.

7 M. Aihara, T. Nagai, J. Matsushita, Y. Negishi and H. Ohya, *J. Chem. Eng. Jpn.*, 1996, **29**, 119.

8 A. Abhat, *Solar Energy*, 1983, **30**, 313.

9 M.N.A. Hawlader, M.S. Uddin and M.M. Khin, *Appl. Energy*, 2003, **74**, 195.

10 A. Sarı and A. Karaipekli, *Mater. Chem. Phys.*, 2008, **109**, 459.

11 F. Frusteri, V. Leonardi, S. Vasta and G. Restuccia, *Appl. Therm. Eng.*, 2005, **25**, 1623.

12 N. Sarier and E. Onder, *Thermochim. Acta*, 2007, **452**, 149.

13 D. Zhao, Q. Huo, J. Feng, B.F. Chmelka and G.D. Stucky, *J. Am. Chem. Soc.*, 1988, **120**, 6024.

14 S. Jun, S.H. Joo, R. Ryoo, M. Kruk, M. Jaroniec, Z. Liu, T. Ohsuna and O. Terasaki, *J. Am. Chem. Soc.*, 2000, **122**, 10712.

15 M. Miyahara and K.E. Gubbins, *J. Chem. Phys.*, 1997, **106**, 2865.

16 A. Watanabe, T. Iiyama and K. Kaneko, *Chem. Phys. Lett.*, 1999, **305**, 71.